NOTES AND CORRESPONDENCE

Aspects of a Rotating Shear Flow over a Mountain Ridge

PETER R. BANNON

Department of Meteorology, The Pennsylvania State University, University Park, Pennsylvania

28 November 1989 and 15 June 1990

ABSTRACT

The effect of a vertical incident wind shear on rotating airflow over a mountain ridge is discussed physically from a variety of perspectives. The apparent paradox that the shear reduces both the vertical displacement of fluid parcels aloft and the mountain anticyclone is resolved. The importance of meridional displacements in representing the static stability field is also demonstrated.

1. Introduction

Several investigators (e.g., Hayes et al. 1987; Bannon and Zehnder 1989) have presented solutions for the problem of rotating, stratified shear flow over a mountain ridge. These solutions indicate that the mountain-induced anticyclone predicted by barotropic theory on the f-plane is weaker in the presence of forward shear (i.e., wind increasing with height). This note seeks to provide a clear physical explanation of this finding. The following discussion uses the quasi-geostrophic model, presented in section 2, of shear flow over a ridge. Such a model is applicable to mountain ranges such as the Rocky Mountains of North America. Sections 3–7 apply thermal, vorticity, static stability, potential vorticity, and omega-equation/**Q**-vector considerations, respectively, in explaining the role of shear.

2. The model

A zonal flow with a linear vertical wind shear is incident on a mountain ridge. The ridge lies along the y-axis of a Cartesian coordinate system on the f-plane. The stably stratified model atmosphere is semi-infinite in the vertical direction. The flow is assumed to be steady, adiabatic, inviscid, Boussinesq, two-dimensional, and quasi-geostrophic. The governing equations are

$$-fv = -\partial\phi/\partial x, \tag{2.1}$$

$$dv/dt = -fu_a, \tag{2.2}$$

$$\partial\phi/\partial z = g(\theta'/\theta_0), \tag{2.3}$$

$$(\partial u_a/\partial x) + (\partial w/\partial z) = 0, \tag{2.4}$$

$$d\theta'/dt = -w(d\theta_s/dz) - v(d\Theta/dy), \tag{2.5}$$

where

$$d/dt = U(z)(\partial/\partial x). \tag{2.6}$$

Here

$$U(z) = U_0 + \alpha z, \tag{2.7}$$

is the incident geostrophic wind with surface speed U_0 and shear α. The total geopotential, Φ,

$$\Phi = -fU(z)y + \phi(x, z), \tag{2.8}$$

is the sum of the potential associated with the incident flow (2.7) and the mountain induced contribution ϕ. The total (potential) temperature, θ, is

$$\theta = \theta_0 + (d\theta_s/dz)z + (d\Theta/dy)y + \theta'(x, z), \tag{2.9}$$

where θ_0 is a reference temperature and $d\theta_s/dz$ (>0) describes the uniform basic state stratification. Here, θ' is the perturbation temperature, and

$$d\Theta/dy = -(\theta_0 f\alpha/g) \leqslant 0 \tag{2.10}$$

is the constant meridional temperature gradient associated with (2.7) by the thermal wind relation. The notation is standard with $u_a = u_a(x, z)$ denoting the ageostrophic part of the zonal wind.

The boundary conditions require that the flow is bounded at $z = +\infty$ and that

$$w = U(dh/dx) \quad \text{at} \quad z = 0, \tag{2.11}$$

where $h(x)$ is the mountain profile.

The problem posed by (2.1)–(2.5) with (2.11) is readily solved using Fourier transforms. Let the transform $\hat{h}(k)$ of the profile $h(x)$ be defined by

$$h(x) = \int \hat{h}(k)e^{ikx}dk, \tag{2.12}$$

Corresponding author address: Dr. Peter Bannon, Department of Meteorology, Pennsylvania State University, 503 Walker Bldg., University Park, PA 16802.

where k is the wavenumber and the limits of integration are infinite. Then the solution for the mountain induced geopotential is

$$\phi(x, z) = Nf \int \hat{h} e^{ikx} e^{-\lambda z} \left(|k| + \frac{\alpha f}{U_0 N} \right)^{-1} dk, \tag{2.13}$$

where $\lambda = |k|Nz/f$. Here $N = [(g/\theta_0)d\theta_s/dz]^{1/2}$ is the buoyancy frequency. Other flow quantities are readily found from (2.13) using (2.1)–(2.5).

Inspection of (2.13) indicates that the amplitude of the integrand is reduced for the shear ($\alpha > 0$) case compared with the barotropic ($\alpha = 0$) case. Thus, it is clear mathematically that the shear reduces the mountain anticyclone. In order to quantify this result, Fig. 1 plots the relative vorticity, $\zeta = \partial v/\partial x$, at the mountain peak, as a function of the shear. The integrals are evaluated numerically for a Gaussian mountain,

$$h(x) = h_0 \exp[-(x/a)^2], \tag{2.14}$$

of height, h_0, and width, a, whose transform is

$$\hat{h}(k) = h_0 a \exp[-(k^2a^2)/4]/2\sqrt{\pi}. \tag{2.15}$$

The vorticity field for (2.15) may then be written as

$$\zeta = -(Nh_0/a\sqrt{\pi}) \int_0^\infty \frac{\kappa^2 e^{-\kappa^2/4} e^{i\kappa\hat{x} - \kappa\hat{z}}}{[\kappa + \gamma]} d\kappa, \tag{2.16}$$

where $\kappa = ak$, $\hat{x} = x/a$, and $\hat{z} = Nz/fa$ are scaled variables. The sole nondimensional parameter in this problem is γ where

$$\gamma = \alpha f a / U_0 N \tag{2.17}$$

is a measure of the strength of the shear. Note that γ is the change in the incident wind speed relative to its surface value U_0 over one Rossby height, $H_R = fa/N$.

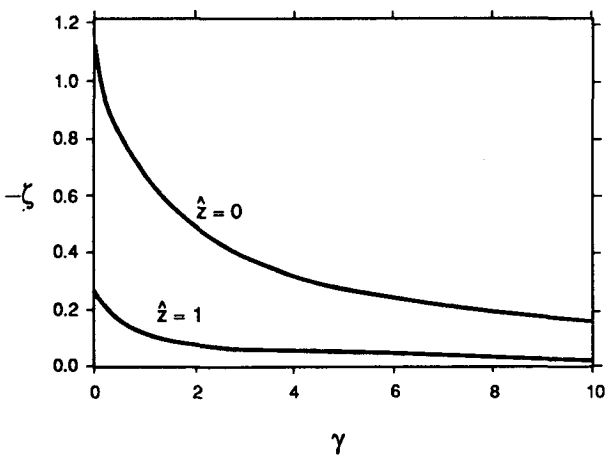

FIG. 1. The anticyclonic vorticity, $-\zeta$, (in units of Nh_0/a) over the mountain top ($x = 0$) as a function of the nondimensional shear, $\gamma = (\alpha fa)/U_0N$, at the surface $\hat{z} \equiv z/H_R = 0$ and at $\hat{z} = 1$, where $H_R = fa/N$ is the Rossby height.

Figure 1 and (2.16) show that the shear reduces the strength of the mountain anticyclone monotonically to zero as $\gamma \to \infty$. The following sections explore the reasons for this reduction.

3. Thermodynamics

The heat equation (2.5) states that the thermal anomaly is governed by adiabatic cooling, for $w > 0$, and by warm air advection, for $v > 0$. At the surface, w is given by (2.11) and fluid parcels are adiabatically cooled as they ascend the mountain to form a cold-core mountain anticyclone. In quasi-geostrophic theory this cooling is the same for both the shear and barotropic cases. Bannon and Zehnder (1989) note that warm air advection partially compensates this cooling in the shear case as parcels are deflected to the north on the windward side of the mountain. The reduced thermal anomaly at the mountain top implies, by integrating the hydrostatic and thermal wind relations downward from infinity where the flow anomalies vanish, weaker geopotential and wind fields.

It is worth noting that the warm advection cannot dominate the adiabatic cooling. If such a situation arose, either the mountain anticyclone would be warm-cored and thus increase with height, thereby violating the boundedness condition, or a warm-core cyclone would be created, thereby satisfying that condition. In the latter case, however, a parcel would be deflected to the south ($v < 0$) on the upslope, and the assumption of strong warm advection would be contradicted.

It is convenient to express θ' in terms of the vertical and meridional displacements of a parcel, denoted by δ and η, respectively. Here they are defined by

$$w = d\delta/dt, \quad v = d\eta/dt. \tag{3.1}$$

Substitution into (2.5) yields

$$\frac{d}{dt}\left(\theta' + \frac{d\theta_s}{dz}\delta + \frac{d\Theta}{dy}\eta \right) = 0. \tag{3.2}$$

Assuming zero thermal anomaly and displacements upstream, (3.2) implies

$$\theta' = -(d\theta_s/dz)\delta - (d\Theta/dy)\eta, \tag{3.3}$$

and vertical displacements produce negative anomalies while meridional displacements produce warm anomalies for the shear case ($d\Theta/dy < 0$).

Figures 2 and 3 show the displacements δ and η, respectively, as a function of position x at the surface ($\hat{z} = 0$) and aloft ($\hat{z} = 1$) for $\gamma = 0$ and 1. The η-field has a logarithmic singularity when $\gamma = 0$, implying an infinite meridional displacement. Since $\eta = \phi/fU$, this singularity corresponds to the well-known singularity for the geopotential in two-dimensional rotating flow. Here, results for $\gamma = 10^{-6}$ are presented. The figures indicate that the shear reduces the amplitude of η and of δ aloft. Thus the thermal anomaly aloft is reduced

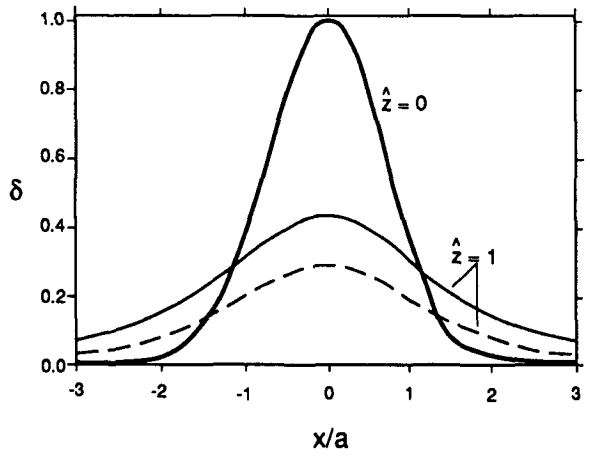

FIG. 2. Vertical displacement, δ, (in units of the mountain height h_0), of a fluid parcel as a function of distance, x, from the mountain crest for $\hat{z} = 0$ and $\hat{z} = 1$. The solid curve denotes the barotropic ($\gamma = 0$) case; the dashed curves the shear ($\gamma = 1$) case. At $\hat{z} = 0$, the vertical displacement is the same in each case and corresponds to the mountain height.

by the shear due to the presence of warm advection and to a reduction in the adiabatic cooling. This behavior results in a shallower anticyclone in the shear case (see Bannon and Zehnder 1989, Fig. 4).

4. Vorticity dynamics

The evolution of the vorticity field is described by the equation

$$d\zeta/dt = f(\partial w/\partial z), \qquad (4.1)$$

which states that only stretching of the planetary vorticity can produce changes in the relative vorticity. Since Fig. 1 displays a reduction in $|\zeta|$ as the shear increases, (4.1) implies that the stretching is also reduced by the shear. This feature is consistent with the form of the solution for the vertical motion field:

$$w = \int ik\hat{U}\hat{h}e^{ikx}e^{-\lambda z}W(k, z)dk, \qquad (4.2)$$

where

$$W(k, z) = [|k| + \alpha f/NU(z)][|k| + \alpha f/NU_0]^{-1}.$$

It is, at first glance, rather surprising then that the shear has reduced the vertical displacements of parcels aloft (see Fig. 2). It is incorrect to infer from Fig. 2 that the vortex squashing is enhanced by the shear. Using (3.1a), the stretching term may be written as

$$f\frac{\partial w}{\partial z} = fU(z)\frac{\partial}{\partial z}\left(\frac{\partial \delta}{\partial x}\right) + f\alpha\frac{\partial}{\partial x}\delta. \qquad (4.3)$$

Since $\partial\delta/\partial x$ is the slope of a parcel trajectory in the x–z plane, the terms on the right-hand-side of (4.3) may be called the differential slope and shear-slope term, respectively. For barotropic flow only, the differential slope mechanism can produce vorticity changes; for shear flow, both mechanisms can.

Figure 4 provides an example of each mechanism. Figure 4a displays a case of stretching by pure differential slope. Here the shear is zero [$\alpha = 0$ and $U(z) = U_0$] but the slope of the parcel trajectory increases with height, $(\partial^2\delta/\partial z\partial x) > 0$. As the fluid column moves, it remains upright as its base and lid are separated vertically. In Fig. 4b, for the case of pure shear-slope, there is shear but the slope of the parcel trajectory is uniform with height. The subsequent tilting of the fluid column again leads to a vertical separation of its base and lid.

As a fluid column ascends the mountain in the barotropic case (Fig. 5a), it first stretches slightly since the

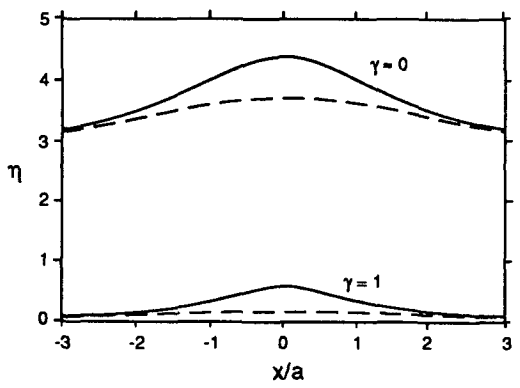

FIG. 3. Meridional displacement, η, (in units of Nh_0a/U_0) of a fluid parcel from its upstream value as a function of distance, x, from the mountain crest. The upper and lower pair of curves denote the barotropic ($\gamma = 10^{-6} \approx 0$) and the shear ($\gamma = 1$) case, respectively. The solid and dashed curves correspond to parcels with $\hat{z} = 0$ and 1, respectively.

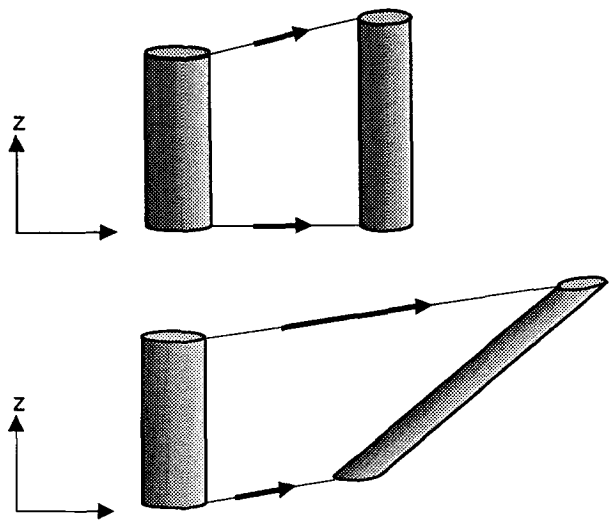

FIG. 4. Examples of vortex stretching of a fluid column by (a) the differential slope and (b) the shear mechanism. The thin solid lines denote the displacement of the column lid and base.

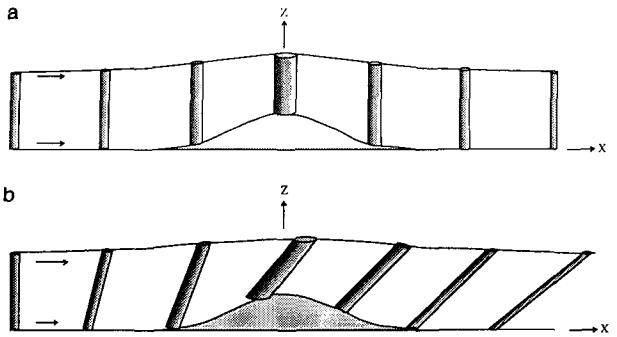

FIG. 5. Schematic projection onto the zonal (x–z) plane of a fluid column crossing a mountain ridge for (a) the barotropic ($\gamma = 0$) and (b) the shear ($\gamma > 0$) case.

slope increases slightly with height, $\partial^2\delta/\partial z\partial x > 0$, far upstream of the mountain and generates weak cyclonic vorticity (Buzzi and Tibaldi 1976). Near the mountain, the slope strongly decreases with height, the column shrinks, and anticyclonic vorticity resides over the mountain crest. The inverse process occurs on the lee-side. In the shear case (Fig. 5b), the cyclonic vorticity on the sides is larger (e.g., Bannon and Zehnder 1989) because the differential slope mechanism is enhanced [both by a larger $\partial^2\delta/\partial z\partial x$ (see Fig. 2) and, aloft, by a larger wind] and the shear-slope term acts to generate positive vorticity. Near the mountain top, the differential slope mechanism becomes negative and dominates the shear-slope term to produce a mountain anticyclone. The positive contribution of the shear-slope mechanism on the windward side, however, results in a weaker anticyclone.

It is important to note that the vertical separation of the δ-surfaces in Fig. 5b is not the total (inverse) measure of the column's vorticity. The vorticity equation (4.1) with (4.3) may be written as

$$\frac{d}{dt}\left(\zeta - f\frac{\partial\delta}{\partial z} - f\frac{\alpha\delta}{U}\right) = 0, \tag{4.4}$$

which implies

$$\zeta = +f\{(\partial\delta/\partial z) + [\alpha\delta/U(z)]\}. \tag{4.5}$$

Thus, an increase in vorticity from its upstream value of zero is associated with an increase in the displacement of a fluid parcel with height and with an upward displacement of the parcel in a shear flow ($\alpha > 0$). Even though $\partial\delta/\partial z$ is more negative for the shear case, the δ-effect in (4.5) compensates and a weaker anticyclone forms.

5. Static stability dynamics

In a quasi-geostrophic fluid, changes in the static stability field are closely related to those of the vorticity field, ζ. Differentiation of the heat equation (2.5) with respect to height produces an equation for the time evolution of the static stability anomaly, $\partial\theta'/\partial z$,

$$\frac{d}{dt}\left(\frac{\partial\theta'}{\partial z}\right) = -\frac{d\theta_s}{dz}\left(\frac{\partial w}{\partial z}\right). \tag{5.1}$$

Thus, only vertical convergence can increase the static stability of a quasi-geostrophic parcel, and the source term on the right-hand side can be interpreted in terms of the vertical displacement in a manner analogous to that of section 4 for the vortex stretching term:

$$\frac{\partial\theta'}{\partial z} = -\frac{d\theta_s}{dz}\left[\frac{\partial\delta}{\partial z} + \frac{\alpha\delta}{U(z)}\right]. \tag{5.2}$$

The presence of shear, therefore, reduces the magnitude of the static stability increase over the mountain top.

It is important to note that terms associated with the tilting of horizontal thermal gradients into the vertical, namely,

$$\frac{\partial U}{\partial z}\frac{\partial\theta'}{\partial x} + \frac{\partial v}{\partial z}\frac{\partial\Theta}{\partial y}, \tag{5.3}$$

cancel by the thermal wind relation. While (5.1) indicates that vertical convergence produces static stability changes, (3.3) implies

$$\frac{\partial\theta'}{\partial z} = -\frac{d\theta_s}{dz}\frac{\partial\delta}{\partial z} - \frac{d\Theta}{dy}\frac{\partial\eta}{\partial z}, \tag{5.4}$$

and the static stability anomalies are associated with vertical variations in both δ and η. We note that (5.2) and (5.4) imply that δ and $\partial\eta/\partial z$ are related by the relation

$$\delta = \frac{fU}{N^2}\frac{\partial\eta}{\partial z}. \tag{5.5}$$

Figure 6 schematically describes the role of the differential displacements on the static stability of the flow. In the barotropic case (Fig. 6a), the fluid column undergoes a large (i.e., infinite) northward displacement as it ascends the ridge. Consistent with Figs. 2 and 3, the column's base is lifted higher and deflected further north than its lid. Since the ambient isentropic surfaces are horizontal ($d\Theta/dy = 0$), the increase in static stability is only associated with the differential vertical displacement, $\partial\delta/\partial z$. In the shear case (Fig. 6b), the column undergoes a smaller (i.e., finite) meridional displacement with a similar differential meridional displacement of its lid and base (Fig. 3). The column's base is lifted as high as that in the barotropic case but not its lid (Fig. 2). Nonetheless, the increase in the static stability for the shear case is less.

6. Potential vorticity thinking

In this adiabatic inviscid flow, the potential vorticity, q, where

$$q = \zeta + \frac{f_0}{(d\theta_s/dz)}\frac{d\theta'}{dz}, \tag{6.1}$$

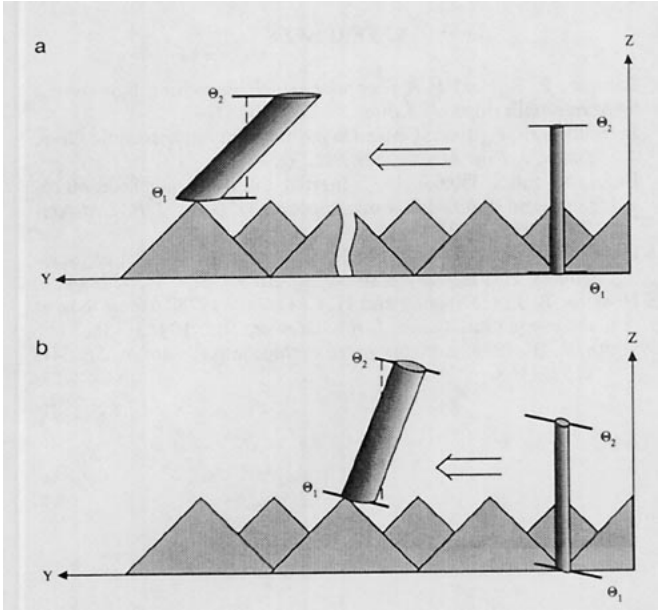

FIG. 6. Schematic projection onto the meridional (y–z) plane of a fluid column crossing an idealized mountain ridge for (a) the barotropic ($\gamma = 0$) and (b) the shear ($\gamma > 0$) case. In each panel the column on the right is incident on the ridge and is differentially deflected to the left as it ascends the mountain. Since the column trajectory is steeper than the tilt of the ambient isentropes (heavy solid lines), the columns at the mountaintop are cold relative to their surroundings. The dashed line measures the vertical separation of the isentropic surfaces following (5.4), and is an inverse measure of the static stability of the column. The break in the mountain chain in (a) symbolizes the infinite meridional displacement in the barotropic case.

is conserved

$$dq/dt = 0. \tag{6.2}$$

In particular, $q = 0$. Following Bretherton (1966), the surface potential temperature gradient can be interpreted as a gradient in a surface charge of potential vorticity. Combining (3.2) evaluated at the surface and (6.2) yields an expression for this generalized potential vorticity

$$\frac{d}{dt}\left[q + \left(\frac{d\theta_s}{dz}\right)^{-1} f_0\delta(z)\left(\theta' + h\frac{d\theta_s}{dz}\right)\right] + \beta_{\text{eff}} v = 0, \tag{6.3}$$

where

$$\beta_{eff} = f_0\delta(z)\frac{d\Theta}{dy}\left(\frac{d\Theta_s}{dz}\right)^{-1}$$

is an effective beta associated with the surface temperature gradient. Here $\delta(z)$ is the Dirac delta function. Since $\beta_{\text{eff}} < 0$ in the shear case, the northward deflected flow on the upstream side of the mountain acts to generate positive relative vorticity and thus reduce the strength of the mountain anticyclone. Note that action of this effective β can only partially compensate the mountain anticyclone. Overcompensation would lead to a mountain cyclone that would be inconsistent with the northward flow upstream of the obstacle.

7. Omega equation

The diagnostic equation for the vertical motion field is

$$(N^2\partial^2 w/\partial x^2) + (f^2\partial^2 w/\partial z^2) = 2f\alpha(\partial\zeta/\partial x) \equiv 2(\partial Q/\partial x), \tag{7.1}$$

where $Q = f\alpha\partial v/\partial x$ is the zonal component of the **Q**-vector (Hoskins et al. 1978). Equation (7.1) must be solved subject to the lower boundary condition

$$w = U_0(\partial h/\partial x) \quad \text{at} \quad z = 0. \tag{7.2}$$

The full solution for w is the sum of the boundary contribution due to (7.2) and to the interior forcing term as the right-hand side of (7.1). The boundary term forces rising motion at the surface upstream of the mountain and sinking downstream, which is the same for both the barotropic and shear case. The interior forcing, present only in the shear ($\alpha > 0$) case, contributes a similar vertical motion pattern aloft (see Fig. 9 of Bannon and Zehnder). The additional rising motion upstream of the mountain in the shear case results equally from warm air advection, i.e.,

$$-\frac{\partial^2 v}{\partial x^2}\left(\frac{g}{\theta_0}\frac{d\Theta}{dy}\right)$$

and positive differential vorticity advection, i.e.,

$$f\frac{\partial U}{\partial z}\frac{\partial\zeta}{\partial x}.$$

Each of these processes contributes half of the forcing term in (7.1). Together they represent the quasi-geostrophic tendency to destroy thermal wind balance. [The balance is maintained, however, by the action of the ageostrophic motion.]

The **Q**-vectors point upstream and have a negative extremum over the mountain top where the relative vorticity is a minimum. Farther upstream and downstream, **Q** displays weak positive extrema associated with the small far-field cyclonic vorticity. The **Q**-field is convergent on the upslope and divergent on the downslope side of the mountain.

Thus, the rising motion upstream of the mountain aloft is greater for the shear case. Consequently, the amplitude of $\partial w/\partial z$ is less and, by (4.1), the vortex squashing is reduced in the shear case, leading to a weaker mountain anticyclone.

8. Conclusions

A variety of approaches have been taken to explain the effect of shear on steady, rotating, stratified flow over topography in the quasi-geostrophic limit. Together they illustrate the internal consistency of the quasi-geostrophic solution. It is noted that the qualitative discussion presented here is also consistent with the semigeostrophic results of Bannon and Zehnder (1989) and are also applicable to the case of backward

shear (wind decreasing with height). There $\beta_{eff} > 0$ and stationary lee waves comprise part of the solution (Smith 1986). The backward and forward shear cases are therefore analogous to eastward and westward barotropic mountain flow on a beta plane.

Acknowledgments. The author benefited from discussions with John H. E. Clark and Huw C. Davies (who suggested section 7) and from questions by Dale R. Durran, David P. Dempsey, and James Wilczak on an earlier version of Fig. 6. This material is based upon work supported by the National Science Foundation under Grant ATM-8813315.

REFERENCES

Bannon, P. R., and J. A. Zehnder, 1989: Baroclinic flow over a mountain ridge. *J. Atmos. Sci.*, **46,** 703–714.

Bretherton, F. P., 1966: Critical layer instability in baroclinic flows. *Quart. J. Roy. Meteor. Soc.*, **92,** 325–334.

Buzzi, A., and S. Tibaldi, 1977: Inertial and frictional effects on rotating and stratified flow over topography. *Quart. J. Roy. Meteor. Soc.*, **103,** 135–150.

Hayes, J. L., R. T. Williams and M. A. Rennick, 1987: Lee cyclogenesis. Part I: Analytic studies. *J. Atmos. Sci.*, **44,** 432–442.

Hoskins, B. J., I. Draghici and H. C. Davies, 1978: A new look at the ω-equation. *Quart. J. Roy. Meteor. Soc.*, **104,** 31–38.

Smith, R. B., 1984: A theory of lee cyclogenesis. *J. Atmos. Sci.*, **41,** 1159–1168.